ARTICLE

BIOTECHNOLOGY and BIOENGINEERING

Microporous Cell-Laden Hydrogels for Engineered Tissue Constructs

Jae Hong Park,[1,2,3] Bong Geun Chung,[1,2,4] Won Gu Lee,[1,2] Jinseok Kim,[1,2] Mark D. Brigham,[1,2] Jaesool Shim,[1,2,5] Seunghwan Lee,[1,2] Chang Mo Hwang,[1,2] Naside Gozde Durmus,[6] Utkan Demirci,[1,2] Ali Khademhosseini[1,2]

[1]Department of Medicine, Center for Biomedical Engineering, Brigham and Women's Hospital, Harvard Medical School, 65 Landsdowne Street, Rm 265, Cambridge, Massachusetts 02139; telephone: 617-768-8395; fax: 617-768-8477; e-mail: alik@rics.bwh.harvard.edu

[2]Harvard-MIT Division of Health Sciences and Technology, Massachusetts Institute of Technology, Cambridge, Massachusetts 02139

[3]National Nano Fab Center (NNFC), Daejon, Korea

[4]Department of Bionano Engineering, Hanyang University, Ansan, Korea

[5]Department of Mechanical Engineering, Yeungnam University, Gyeongsan, Korea

[6]Department of Biomedical Engineering, Boston University, Massachusetts

Received 24 August 2009; revision received 17 December 2009; accepted 30 December 2009

Published online 20 January 2010 in Wiley InterScience (www.interscience.wiley.com). DOI 10.1002/bit.22667

ABSTRACT: In this article, we describe an approach to generate microporous cell-laden hydrogels for fabricating biomimetic tissue engineered constructs. Micropores at different length scales were fabricated in cell-laden hydrogels by micromolding fluidic channels and leaching sucrose crystals. Microengineered channels were created within cell-laden hydrogel precursors containing agarose solution mixed with sucrose crystals. The rapid cooling of the agarose solution was used to gel the solution and form micropores in place of the sucrose crystals. The sucrose leaching process generated homogeneously distributed micropores within the gels, while enabling the direct immobilization of cells within the gels. We also characterized the physical, mechanical, and biological properties (i.e., microporosity, diffusivity, and cell viability) of cell-laden agarose gels as a function of engineered porosity. The microporosity was controlled from 0% to 40% and the diffusivity of molecules in the porous agarose gels increased as compared to controls. Furthermore, the viability of human hepatic carcinoma cells that were cultured in microporous agarose gels corresponded to the diffusion profile generated away from the microchannels. Based on their enhanced diffusive properties, microporous cell-laden hydrogels containing a microengineered fluidic channel can be a useful tool for generating tissue structures for regenerative medicine and drug discovery applications.

Biotechnol. Bioeng. 2010;106: 138–148.

KEYWORDS: microporous; agarose; cell-laden hydrogel; tissue engineering

Introduction

Hydrogels hold great potential as scaffolding materials for a number of biological applications such as regenerative medicine, drug discovery, and biosensors as they can provide physiological environments with characteristics such as high water content, high porosity, and mechanical support (Khademhosseini and Langer, 2007; Peppas et al., 2006). Hydrogels have been used for tissue engineering field for a number of tissue types, including bone (Burdick and Anseth, 2002; Burdick et al., 2002, 2003), cartilage (Bryant and Anseth, 2003), liver (Liu Tsang et al., 2007), brain

J.H.P. and B.G.C. designed and performed the experiments, and analyzed the data. W.G.L. fabricated agarose channels and analyzed the data. J.S.K. conceived the methodology for creating micropores and analyzed confocal images. M.B. measured the porosity and characterized mechanical strength. J.S. characterized diffusion coefficient and profiles. S.H.L. synthesized biomaterials, characterized porosity, and analyzed the data. C.H. performed cell experiments and analyzed the data. G.D. created and characterized pores within agarose gels using sucrose mixtures. U.D. helped in analysis of the data. A.K. supervised the work and conceived of the idea. All authors read and wrote the paper.

Jae Hong Park and Bong Geun Chung equally contributed to this work.

Jinseok Kim's present address is Nanobio Center, Korea Institute of Science and Technology (KIST), Seoul, Korea.

Correspondence to: A. Khademhosseini

Contract grant sponsor: The National Institutes of Health
Contract grant number: DE019024; HL092836; EB007249
Contract grant sponsor: US Army Core of Engineers
Contract grant sponsor: The Charles Stark Draper Laboratory
Contract grant sponsor: Korea Research Foundation Grant (MOEHRD)
Contract grant number: KRF-2007-357-D00101

(Bakshi et al., 2004; Ford et al., 2006; Tian et al., 2005; Woerly, 1993), and others (Changez et al., 2004; Elisseeff et al., 2000; Mann et al., 2001). Due to their excellent properties, hydrogels derived from natural sources (i.e., collagen, hyaluronic acid (HA), chitosan, alginate, and agarose) or synthetic materials (i.e., polyethylene glycol (PEG)) have been extensively used for various tissue engineering applications (Khademhosseini et al., 2006; Lee and Mooney, 2001; Wu et al., 2008).

Agarose, a temperature-sensitive and water soluble hydrogel, is a polysaccharide extracted from marine red algae (Aymard et al., 2001) and is used as a cell culture substrate (Uludag et al., 2000). The mechanical properties of agarose gels can be controlled by gelling temperatures and curing times (Aymard et al., 2001). Furthermore, the diffusion properties of macromolecules such as proteins, polymer beads, and DNA within agarose gels have been characterized by using fluorescence based methods (Pluen et al., 1999) and movement of nanoparticles (Fatin-Rough et al., 2004; Labille et al., 2007). Biocompatible agarose gel has been used for the cell encapsulation and *in vivo* transplantation applications (Rahfoth et al., 1998; Uludag et al., 2000).

Porous structures in biomaterials are potentially useful for mimicking native tissues. Pores improve protein transport and diffusion in agarose gels. To make porous scaffolds, several methods have been previously developed. For example, colloidal suspension was used to create pores within Hydroxyapatite scaffolds scaffolds (Cordell et al., 2009). The mechanical bending and compression analysis of this scaffold has shown that strength of the bulk microporous scaffold with smaller micropore sizes was higher that scaffold with larger micropore sizes. This was consistent with reported results for other porous materials (Bignon et al., 2003; Sopyan et al., 2007). Also, poly(methyl methacrylate) (PMMA) beads were used to generate microporous structures within fibrin scaffolds (Linnes et al., 2007). To create micropores within scaffolds, PMMA beads were removed by using toxic chemical processes.

Sucrose is a promising crystal as a pore or particle forming agent (Huang et al., 2003; Kwok et al., 2000). It has been used to create particles and pores within polylactideglycolic acid (PLGA) sponges during a gas foaming process (Huang et al., 2003). The elastic modulus of gas-foamed PLGA sponges was decreased with increasing sucrose concentrations. In addition to sucrose crystal leaching method, salt crystals have been previously used to create interconnected pores within polymeric scaffolds (Murphy et al., 2002). Porous PLGA scaffolds were fabricated by solvent casting/particulate leaching or gas foaming leaching methods using a salt. Fusion of salt crystals in the solvent casting process enhanced pore interconnectivity within polymeric scaffolds. The pore size was controlled by using NaCl microparticles. The mechanical properties (i.e., compressive modulus) of scaffolds were strongly dependent on salt fusion and processes, such as solvent casting and gas foaming. Although these methods enable the control of mechanical properties of scaffolds, they have potential limitations, such as the inability directly encapsulate the cells in the materials and the use of toxic chemicals.

With agarose gels, several chemical methods have also been used to create pores (Shi et al., 2005; Zhou et al., 2006). For example, pores have been made by water-in-oil emulsification by using solid granules of calcium carbonate (Shi et al., 2005). Metal oxides have also been used to fabricate macropores within agarose gels (Zhou et al., 2006). However, these methods to create pores within agarose gels can not be used to fabricate cell-laden hydrogels. Cell-laden hydrogel microfluidic devices can mimic the 3D microenvironment of native tissues (Cabodi et al., 2005; Choi et al., 2007; Gillette et al., 2008; Golden and Tien, 2007; Hwang et al., 2008; Ling et al., 2007; Song et al., 2009). The integration of microfabricated devices and biocompatible hydrogels offers the potential for recreating the spatial complexity and diffusion properties of macromolecules. We have previously developed a cell-laden agarose microfluidic system and analyzed the diffusion profiles of molecules from the microchannels (Ling et al., 2007). Given this feature, we hypothesize that the ability to create micropores within the gels around the microchannels may provide potential improvements in biomolecular diffusion and oxygen transport.

In this article, we describe a method to fabricate a cell-laden agarose gel system containing engineered constructs with a microvascular structure and micropores that are created by dissolving sucrose crystals without the use of any organic solvents. For this purpose, we developed the porous cell-laden agarose fluidic device and characterized the physical and mechanical properties of agarose gels with various micropores. We also analyzed the viability of hepatic cells encapsulated within agarose gels. Therefore, this porous cell-laden agarose gel system integrated with a microvascularized channel could be a potentially useful tool to study complex cell–microenvironment interactions and mimic microarchitectures of native tissues.

Materials and Methods

Fabrication of the Microporous Cell-Laden Agarose Gels

We fabricated microporous cell-laden agarose gels containing a microengineered channel as shown in Figure 1. Briefly, sucrose crystals (200 μm in diameter) at varying concentrations of 0, 100, and 200% (w/v) were mixed with 1 mL of the cell suspension (10^7 cells/mL^{-1}) and an additional 1 mL of 6 wt.% agarose solution (Sigma–Aldrich, St. Louis, MO, USA) at 40°C. The initial temperature for sample preparation was 25, 37, and 40°C for sucrose crystals, cell suspension, and agarose solution respectively. Cells were only exposed to 40°C agarose solution for a short time and were cooled down to 4°C after mixing with cell suspension

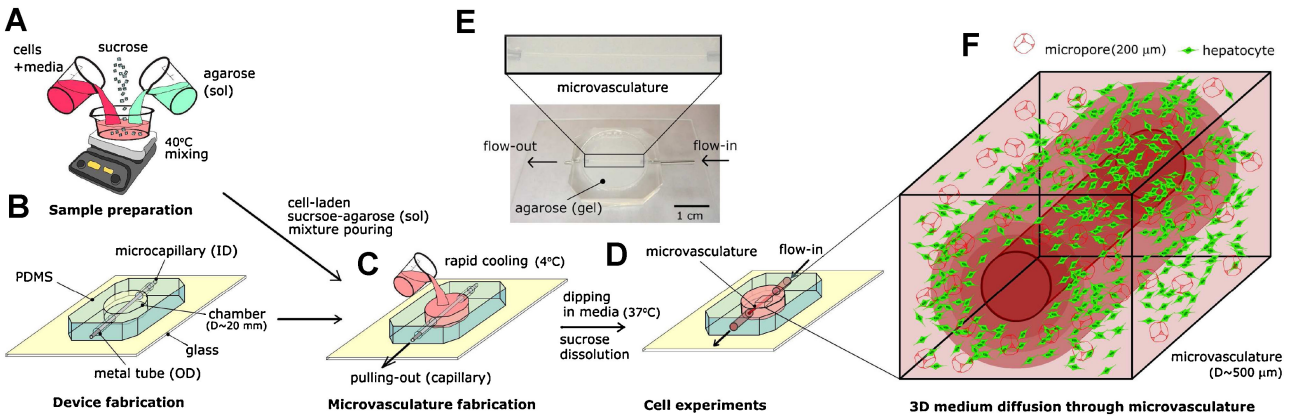

Figure 1. Schematic of the fabrication process for cell-laden hydrogels containing micropores and a microchannel. **A**: Sample preparation: Sucrose crystals (50–200 wt.%), cells (10^7 cells mL^{-1}) and agarose (6 wt.%) solution were mixed at 40°C. **B**: Device fabrication: The mixture was cured within a PDMS cylindrical mold containing a microneedle connected between two metal tubes on PDMS side walls. **C** and **D**: Fabrication of the microengineered hydrogels: When the mixture was confined in the PDMS mold, a microneedle was removed from the PDMS mold to create the microchannel for the microvascularized structure. **E** and **F**: Cell culture in a device: Hepatic cells encapsulated within microporous agarose gels were cultured for 5 days within a fluidic device that could provide continuous medium perfusion. [Color figure can be seen in the online version of this article, available at www.interscience.wiley.com.]

and sucrose crystals as shown in Figure 1A. After mixing, the mixture was poured into a cylindrical poly(dimethylsiloxane) (PDMS) mold (2 cm diameter, 1 cm thick). To generate the hydrogel microchannel, a microneedle (0.38, 0.6 mm inner and outer diameter) was inserted in the middle of the PDMS side walls as a microcapillary (Fig. 1B). The entire molds were then placed either at 25°C for natural gelation or 4°C for rapid gelation (Fig. 1C). After the agarose gelation (~ 20 min), the microneedle was removed from the PDMS mold to create the microchannel (Fig. 1C and D) and the cell-laden agarose gel was immersed within cell culture medium at 37°C to dissolve the sucrose. The sucrose-leached medium in the bath was replaced with fresh medium every 10 min. After 2 h, the sucrose crystals remained within the agarose gels were completely removed (Fig. 1E). For the continuous medium perfusion in the agarose microchannel, polyethylene tubing (1/16 inch inner diameter) was connected to metal tubes in PDMS molds. The culture medium was delivered into the microchannel by using a syringe pump ($2\,\mu L\,min^{-1}$). Hepatic cells encapsulated within microporous agarose gels were cultured for 5 days in vitro (Fig. 1F).

Hepatic Cell Culture and Cell Viability

The hepatocelluar carcinoma cell line (HepG2) was purchased from American Tissue Type Collection (ATTC). All tissue culture components were purchased from Gibco-Invitrogen, CA, unless otherwise indicated. Culture medium for HepG2 cells consisted of Dulbecco's Modified Eagle Medium (DMEM) with 10% (v/v) fetal bovine serum (FBS), and 1% penicillin–streptomycin. Cells cultured in a tissue culture flask were fed by changing the medium every other day and were passaged when 90% confluency was reached. To analyze the viability of cells cultured within microporous agarose gels, a live/dead assay was used (Invitrogen, Carlsbad, CA, USA).

After culturing for 5 days, tubings for medium perfusion were disconnected and cell-laden agarose gels were cut (1 cm × 1 cm × 1 cm) by a knife for the cell viability test. These cell-laden agarose gels were subsequently incubated in 2 μM calcein-AM and 4 μM ethidium homodimer for 10 min (37°C, 5% CO_2). Live (green) and dead (red) cells around the microchannel of cell-laden agarose gels were analyzed by a fluorescence microscope. For the medium perfusion experiment, we analyzed the cross-sectional images of the microchannel in agarose gels. For the control, we characterized cell viability at a depth of 500 μm from agarose gel surface. Cell viability test was performed three times for each gel.

Image Analysis

Phase contrast and fluorescent images of cells encapsulated within agarose gels were obtained from an inverted microscope (TE 2000; Nikon, Japan). We observed the surfaces of agarose gels within cylindrical PDMS molds (2 cm diameter and 1 cm thick) (Figs. 2A–C and 3 Aa–i). For Figure 3Ag–i, the specimens were cross-sectioned by a razor blade and slightly dried before observation. To observe and identify micropores embedded in agarose gels, we used confocal (LSM 510; Zeiss, Germany) and scanning electron microscope (JSM-6500F; Jeol, Tokyo, Japan). For fluorescent imaging (Fig. 3Aj–l) with the confocal microscope,

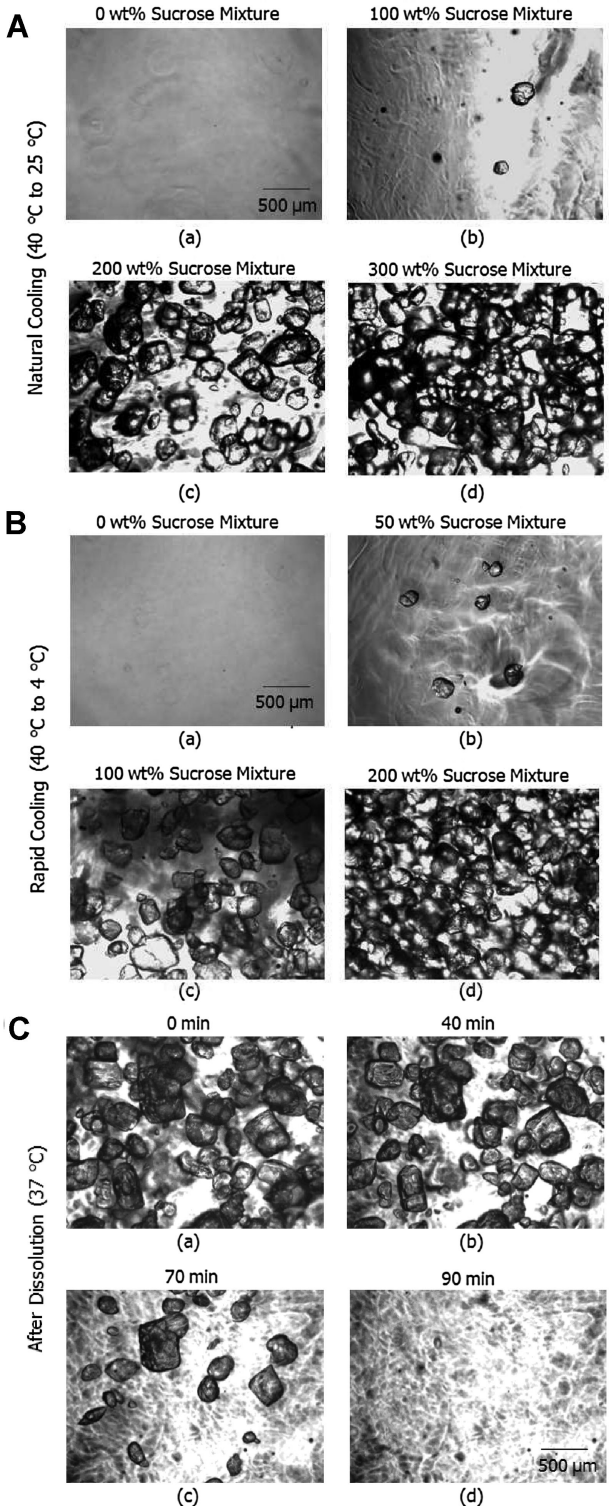

Figure 2. Micrographs of sucrose crystals embedded in agarose gels. **A**: Phase contrast images of sucrose mixtures (0–300 wt.%) after natural cooling (from 40 to 25°C). **B**: Phase contrast images of sucrose mixtures (0–200 wt.%) after rapid cooling (from 40 to 4°C). **C**: Phase contrast images of hydrogels derived from the formulation with 100 wt.% sucrose after dissolution (37°C).

agarose solution was mixed with fluorescein isothiocyanate (FITC)-dextran (0.5 mM, 2000 kDa, Sigma–Aldrich). These phase contrast and fluorescent images for quantifying microporosity were analyzed by using the NIH Image J software with functions for contrast separation, area fractioning, and intensity profiling.

Characterization of Hydrogel Mechanical Properties

We characterized the mechanical stiffness of the gel constructs, which did not contain the cells, by using an Instron 5542 mechanical compression tester at a rate of 20%/min until failure occurred. The compressive modulus of agarose gels containing different sucrose concentrations (0–200 wt.%) was obtained from the linear regime in the 10–15% strain.

Modeling of the Diffusion Profiles in Hydrogels

Diffusion in the extracellular space of cell-laden hydrogels is similar to diffusion in a porous medium. To measure the diffusion properties of agarose gels, the integrative optical imaging (IOI) technique (Nicholson, 2001) could be useful for analyzing macromolecules. As fluorescent dextran diffuses in the agarose gel, the concentration of the fluorescent dye is extracted from the agarose, and the diffusion coefficient is determined. If a representative elementary volume of hydrogel is assumed to be V and the extracellular space is defined as V_0, the diffusion model (Nicholson, 2001) can be expressed as

$$\frac{\partial}{\partial t}\langle C_0\rangle = \hat{D}\nabla^2\langle C_0\rangle + \frac{\langle s\rangle}{\alpha} \tag{1}$$

where the operator is $\nabla^2 = (\partial^2/\partial x_i^2)$, C_0 is the concentration in the extracellular space, s is the source density, α is the porosity defined in the porous medium as (V_0/V), the operator $\langle\rangle$ is space average, and $\hat{D} = D \cdot \hat{K}$ is the effective diffusion coefficient of the hydrogel which is a second-order tensor. The tensor $\hat{K}$ is a reciprocal proportion to the tortuosity of the hydrogels. If the hydrogels are uniform in the space of interest, the tortuosity $(\hat{K})$ is simplified as a scalar in the inverse ratio to the square of tortuosity $(1/\lambda^2)$. In addition, the diffusion equation in the extracellular space could be described in a free medium as follows (Nicholson and Phillips, 1981):

$$\frac{\partial}{\partial t}C = \hat{D}\nabla^2 C + \frac{s}{\alpha} \tag{2}$$

The equation is simplified by dropping the term (s) because there is no source density in the extracellular space.

$$\frac{\partial}{\partial t}C = \hat{D}\nabla^2 C \tag{3}$$

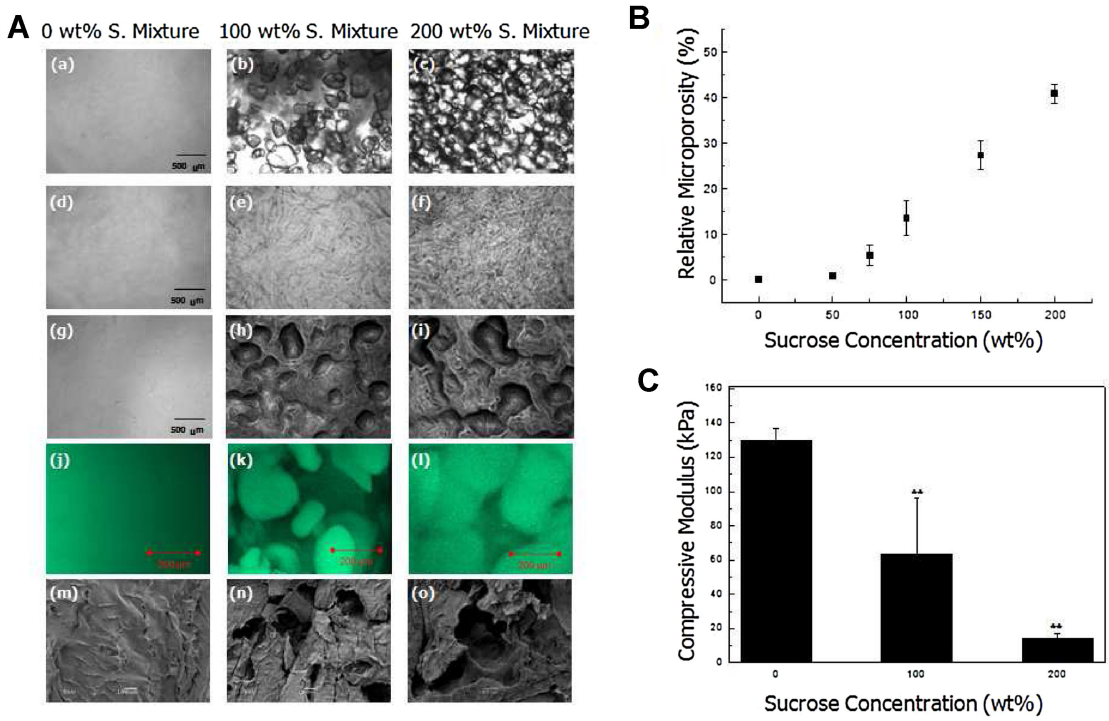

Figure 3. Microporosity and mechanical stiffness of hydrogels. **A**: Images of microporosity: Phase contrast images of sucrose crystals (0–200 wt.%; **a**–**c**), sucrose crystals dissolved within agarose gels (**d**–**f**), and cross-section images of agarose gels containing micropores (**g**–**i**). Confocal microscope images (**j**–**l**) and SEM images (**m**–**o**) of microporosity within agarose gels. **B**: Microporosity in agarose gels with different sucrose concentrations. The percentage of the microporosity is directly proportional to sucrose concentrations. **C**: Mechanical stiffness of agarose gels with sucrose concentrations. Compressive moduli were inversely proportional to sucrose concentrations. Every quantification of the above data was performed five times for each condition. [Color figure can be seen in the online version of this article, available at www.interscience.wiley.com.]

Note that the diffusion coefficient $(\hat{D})$ is a vector in a space.

Although non-uniform transport partially brings out the convective term due to inhomogeneous pores, the average intensity is considered as a uniform transport, allowing for the diffusivity in a specimen. In addition, the evaluation of diffusion properties in a static condition is important because diffusion coefficient should be satisfied in a condition, which excludes convection effect due to an infusion rate. In other words, diffusion can be generated by the Brownian motion, which is caused by the concentration difference. In our experiments and simulations, the infusion effect was not considered and the intensity was only measured in the x–y plane of the hydrogel specimen after starting the diffusion of FITC-dextran into an agarose microchannel due to the concentration difference.

Assumption of the Modeling

This model neglects the source density, which contributes to the transient diffusion profiles except the initial concentration of the fluorescent dye. The hydrogel for experiment has a uniform porous size, so that the diffusion coefficient $(\hat{D})$ is considered as constant in a space. In addition, there is no evaporation of the fluorescent dye into the environment during experiment.

Results and Discussion

Morphology and Mechanical Property of Microporous Gels

The microporosity within hydrogels plays a significant role in controlling the delivery of nutrients and oxygen transport to the cells. Micropores were created by leaching sucrose crystals within agarose gels. Sucrose concentration can we be used to control of the percentage of micropres and the resulting mechanical stiffness of hydrogels. During natural cooling from 40 to 25°C for gelation of agarose, hydrogels derived from the formulation with 200 wt.% sucrose contained homogeneous crystals, while sucrose crystals were aggregated in 300 wt.% sucrose (Fig. 2Ac and d).

The gelation was performed by decreasing the temperature from 40 to 25°C (~2 h). However, the 2 h required for the gelation process in hydrogels derived from the

formulation with 200 wt.% sucrose might result in physiologically osmotic shock in an initial stage. The alternative method for addressing this challenge is to decrease the gelation temperature, as solubility of crystals was dominated by the temperature. The gelation time significantly decreased when temperatures were decreased. Here, we used 4°C, which is suitable for rapid gelation while maintaining cell viability. Therefore, we performed rapid cooling to 4°C for fast gelation. For the rapid cooling ($40 \rightarrow 4$°C), the densities of the sucrose crystals in Figure 2B was similar to the half densities of the sucrose crystals during natural cooling ($40 \rightarrow 25$°C) as shown in Figure 2A. Sucrose crystals within hydrogels derived from the formulation with 100 wt.% sucrose were relatively homogeneously distributed, while they were aggregated in hydrogels derived from the formulation with 200 wt.% sucrose. The gelation time was also reduced to 20 min during the rapid cooling to prevent the potential osmotic shock caused from the natural cooling process. Figure 2C shows phase contrast images of hydrogels derived from the formulation with 100 wt.% sucrose, which remains within agarose gels. It was revealed that most sucrose crystals within hydrogels derived from the formulation with 100 wt.% sucrose in the agarose gels were completely dissolved after 90 min.

We identified micropores, which were formed by the sucrose crystals, by using an inverted microscope (Fig. 3Aa–i), a confocal microscope (Fig. 3Aj–l), and a scanning electron microscope (Fig. 3Am–o). As expected, the relatively homogeneous distribution of pores was observed in hydrogels derived from the formulation with 100 wt.% sucrose. In hydrogels derived from the formulation with 200 wt.% sucrose, pores were interconnected due to aggregation of the sucrose crystals. Figures 3Ak and l show that the diameters of the average pores were approximately 200 μm, which is similar to the original size of sucrose crystals. Furthermore, the microporosity was characterized as a function of sucrose concentration (Fig. 3B). Above 50 wt.% of sucrose, the porosity percentage was linearly increased with sucrose concentrations. This result indicates that we can control pore sizes (i.e., single pores with 200 μm diameter and interconnected pores) and porosities by using various sucrose concentrations.

To characterize the effect of sucrose concentrations on the mechanical stiffness of the agarose gels, we performed compressive testing by using an Instron mechanical tester (Fig. 3C). Hydrogels derived from the formulation with 100 wt.% sucrose had a significantly lower compressive modulus (63.6 ± 33.0 kPa) as compared to those from (129.8 ± 7.0 kPa) non-porous agarose gels. Also, the compressive modulus (14.7 ± 3.0 kPa) of hydrogels derived from the formulation with 200 wt.% sucrose was only 15% of that of non-porous agarose gels. These microporosity and mechanical stiffness results demonstrated that percentages of the microporosity were directly proportional to sucrose concentrations, while compressive moduli were inversely proportional to sucrose concentrations. Although hydrogels derived from the formulation with 200 wt.% sucrose contain 40% microporosity, careful mechanical handling is required because they have the lowest compressive modulus. However, hydrogels derived from the formulation with 100 wt.% sucrose show good mechanical robustness and microporosity (15%). Therefore, sucrose concentrations enabled the control of the microporosity and mechanical stiffness, which could prove advantageous for tailoring the hydrogels to match specific tissue types.

The microporous hydrogels derived from 100 wt.% sucrose-leaching show uniform pore sizes that were similar to the original pore size of the initial sucrose crystals. Nonetheless, we observed the relatively large deviation of the compressive modulus (Fig. 3C). This deviation is probably due to small local connectivity among the micropores derived from the sucrose crystals.

Diffusion Profiles From the Microchannel Within Microporous Agarose Gels

Micropores enable the control of diffusion profiles of soluble molecules from the microchannel within agarose gels. We analyzed the diffusion profiles within agarose gels by using a fluorescent dye (FITC-Dextran, 0.25 mM, 20 kDa). In general, FITC-dextran has a similar molecular weight to soluble growth factors associated with metabolism in the body. The channel surface of hydrogels derived from the formulation with 100 wt.% sucrose (Fig. 4Ad) was relatively rough as compared to that of 0 wt.% sucrose mixtures (Fig. 4Ab) due to micropores around the microchannel.

To characterize the diffusion patterns as a function of time at each sucrose concentration, we performed diffusion experiments in a static condition after infusion of FITC-dextran into an agarose microchannel (Fig. 4B). The evaluation of diffusion properties in a static condition is important, because it can exclude the surface roughness effect that may cause non-pure diffusion. As expected, in hydrogels derived from the formulation with 100 and 200 wt.% sucrose (Fig. 4Bd–i), diffusion patterns were not uniform due to micropores around the microchannel. The diffusion coefficient can be defined as the diffusion occurs in a Brownian motion by pure diffusion. Thus, the convective effect by non-uniform pores brings about an undesirable diffusion coefficient. In our experiment, non-uniform transport partially makes convective term due to inhomogeneous pores during the diffusion process. To minimize the convective effect, Nicholson et al. (Nicholson and Tao, 1993; Thorne and Nicholson, 2006) introduced a diffusion model in inhomogeneous environment. In this approach, the average intensity was obtained after $t = 10$ min and was applied to the diffusion Equations (1)–(3). Note that the equations are modified from general pure diffusion equation for averaged pure-diffusion.

We also characterized the spatio-temporal diffusion patterns at each sucrose mixture as a function of distance away from the channel surface (Fig. 4C). The simulation results were in agreement with experimental results of

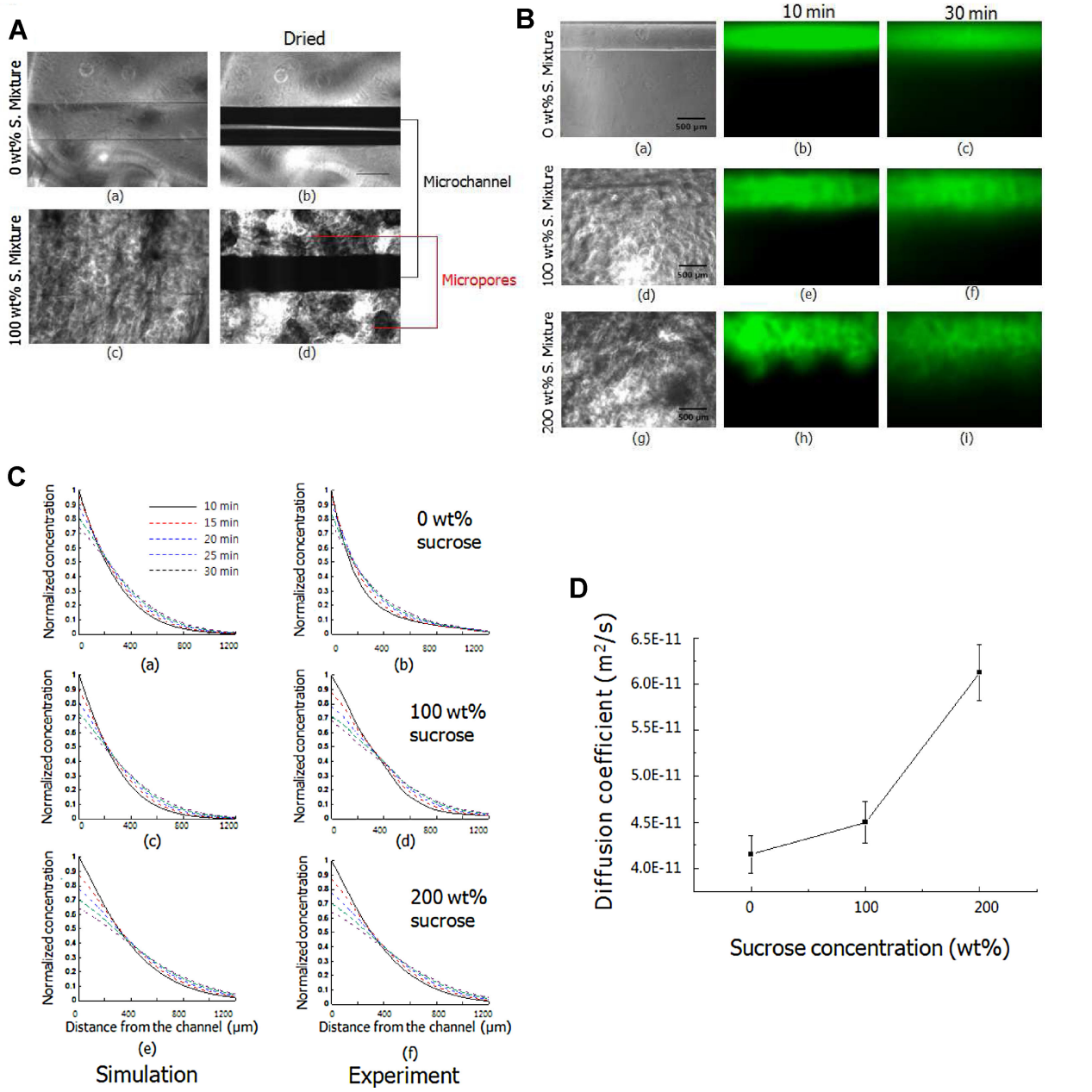

Figure 4. Diffusion profiles in agarose gels containing the microchannel and micropores. **A**: Phase contrast images of a microchannel within agarose gels. **B**: Phase contrast and fluorescent images of diffusion profiles in the agarose microchannels containing different micropores. These diffusion profiles of FITC-dextran (0.25 mM, 20 kDa) were evaluated under static conditions without medium perfusion. **C**: The experimental and theoretical diffusion profiles of the fluorescent dye in the agarose microchannel with different sucrose concentrations (0–200 wt.%) as a function of channel distances. **D**: The characterization of diffusion coefficient within agarose microchannels containing different sucrose concentrations (0–200 wt.%). All experiments and quantification of the above data were performed five times for each condition. [Color figure can be seen in the online version of this article, available at www.interscience.wiley.com.]

diffusion patterns. The diffusion coefficient of the microporous cell-laden agarose gels was calculated by using finite element method (FEM; Comsol, Burlington, MA, USA) and was subsequently compared to the diffusion experiments in agarose gels over time. The simulation for Equation (3) can be conducted in the finite 3D rectangular domain ($2\,\text{mm} \times 1\,\text{mm}$). The channel was located at the center of the specimen and its diameter and length were about 500 μm and 20 mm, respectively. The normalized initial concentrations were applied inside the channel as 1 mM and the boundaries of the specimen were considered to be zero in concentration. The temporal pattern of the diffusion was

calculated inside the gels and channel boundary. The diffusion coefficients were also calculated by simulating hydrogel environments with three different sucrose concentrations (0, 100, and 200 wt.%). As the diffusion is originated from the boundary of specimen, the concentration decreases as a function of channel length and time in Equation (3). The simulations were conducted by changing diffusion coefficient to fit the experimental results of Figures 4Cb, d, and f. In addition, the diffusion profile was extracted from the channel surface to the boundary of the specimen. These results revealed that diffusion velocities increased as porosity increased. Our experimental results are in agreement with the previous studies (Nicholson and Tao, 1993; Thorne and Nicholson, 2006), where the diffusion coefficients of FITC-dextran in agarose gels were reported to be between 4.2 and $13.5 \times 10^{-11}\,m^2\,s^{-1}$. In our experiment, we aimed to confirm the similar pattern for the diffusivity of FITC-dextran in the cell-laden structure under our experimental conditions, such as temperature, hydrogel condition, and perfusion method.

Furthermore, diffusion coefficients of FITC-dextran in the agarose gels were smaller than those in the water ($8 \times 10^{-11}\,m^2\,s^{-1}$ in 20 kDa dextran) (Cornelissen et al., 2008) (Fig. 4D). We found that the diffusion coefficient of FITC-dextran in hydrogels derived from the formulation with 200 wt.% sucrose was approximately 1.5 times higher than that in 0 wt.% sucrose. Therefore, the diffusion coefficient was increased with increasing the sucrose concentrations.

Cell Viability of Microporous Cell-Laden Agarose Gels With a Microchannel

Micropores within cell-laden agarose gels enable the control of cell viability, because medium and nutrients can diffuse through micropores. To study the viability of cells encapsulated within agarose gels containing different micropore sizes, we compared static and medium perfusion culture conditions. Figures 5A and B present fluorescent images of cells and quantitative analysis of cell viability near the surfaces (500 μm deep from the surface) under static culture conditions (no medium perfusion). We found that cell viability in hydrogels derived from the formulation with 100 wt.% sucrose was higher than that in hydrogels derived from the formulation with 0 and 200 wt.% sucrose. Figure 5C shows quantitative analysis of cell viability as a function of distance away from the agarose surface in the static condition. It was revealed that cell viability decreased with increasing distance from the agarose surface. However, at the 2,200 μm distance from the agarose surface, cells in hydrogels derived from the formulation with 100 wt.% sucrose had higher viability (68%) as compared to those in hydrogels derived from the formulation with 0 and 200 wt.% sucrose (44%). This result was similar for cell viability near the surface in the static condition (Fig. 5B), because agarose gels derived from the formulation with 100 wt.% sucrose had 15% micropores and high mechanical stiffness (60 kPa) (Fig. 3B and C). Although hydrogels derived from the formulation with 200 wt.% sucrose was more porous, their mechanical stiffness was approximately 5 times lower than the stiffness of agarose gels with 100 wt.% sucrose. Thus, hydrogels derived from the formulation with 200 wt.%

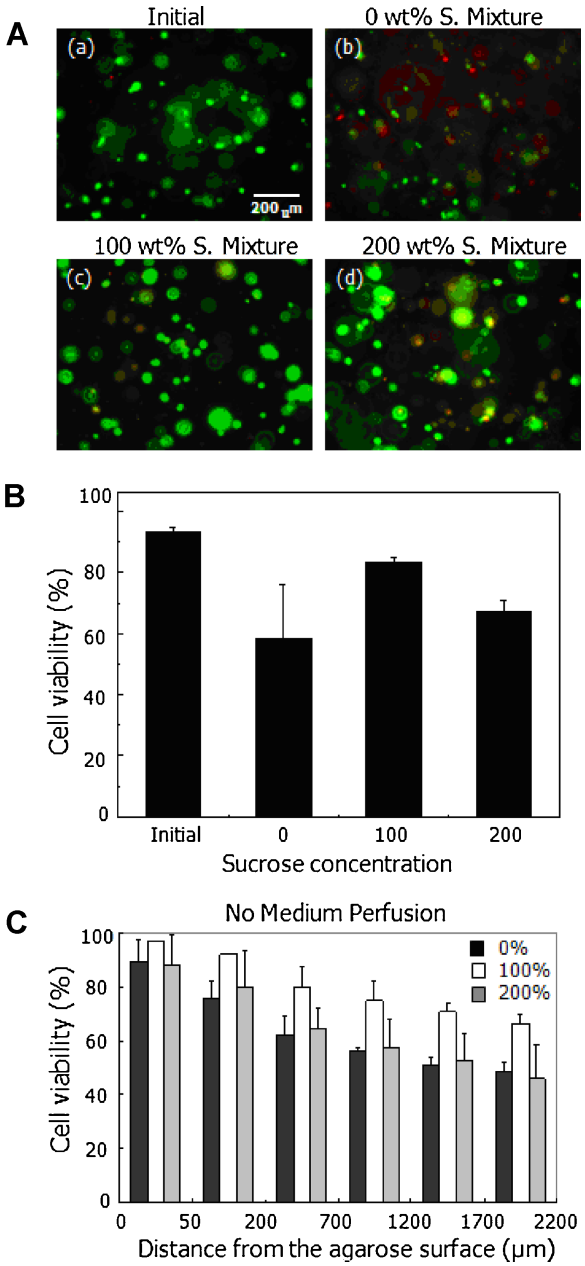

Figure 5. The viability of hepatic cells cultured within agarose gels containing different microporosities without medium perfusion. **A**: Fluorescent images of the cell viability at initial time (**a**), after culturing for 5 days in 0 wt.% (**b**), 100 wt.% (**c**), and 200 wt.% (**d**) sucrose mixtures. **B**: The viability of cells near the surfaces (500 μm deep from the surface) in agarose gels with different sucrose concentrations (0–200 wt.%). Cells were cultured within microporous agarose gels for 5 days in vitro. **C**: The viability of cells cultured for 5 days as a function of the distance away from the agarose gel surface. All quantification of the above data was performed three times for each condition. [Color figure can be seen in the online version of this article, available at www.interscience.wiley.com.]

sucrose might contain weak microstructures (10 kPa). In addition, cell viability in non-porous agarose gels was low, because medium and oxygen could not be easily diffused through smaller pore sizes. We demonstrated that cell viability in hydrogels derived from the formulation with 100 wt.% sucrose was gradually decreased (~30%) as the distance from the agarose surface increased, while cell viability in hydrogels derived from the formulation with 0 and 200 wt.% sucrose was promptly reduced (~45%).

Microporosity within agarose gels can also control diffusion profiles that significantly affect cell viability in the medium perfusion condition. Figure 6A shows cell viability on the cross-sections of the agarose microchannel with 0–200 wt.% sucrose mixtures. Cell viability in hydrogels derived from the formulation with 100 wt.% sucrose (Fig. 6B) was higher than that in hydrogels derived from the formulation with 0 wt.% sucrose at all distances from the medium perfusion channel. Cells cultured near the microchannels showed similar cell viability (80–95%) in different sucrose mixtures. However, the viability in hydrogels derived from the formulation with 200 wt.% sucrose at the 700–2,200 μm distance from microchannels was 10–20% higher than that in non-porous agarose gels, because hydrogels derived from the formulation with 200 wt.% sucrose contained interconnected pores that could easily deliver medium and oxygen to the cells.

For the static culture condition (Fig. 5C), although hydrogels derived from the formulation with 200 wt.% sucrose contained interconnected pores, cell viability was similar to non-porous agarose gels. In contrast, as we applied to medium perfusion in the agarose gel channel with 200 wt.% sucrose, cell viability was higher than non-porous agarose gels (Fig. 6B), because nutrients were easily delivered into the cells through interconnected pores. Thus, the homogeneous porosity derived from 100 wt.% sucrose increased cell viability in the static culture condition, while the interconnected pores made by 200 wt.% sucrose enabled the nutrient delivery into the cells in the medium perfusion condition, resulting in high cell viability. Furthermore, we found that patterns of the cell viability according to the distance away from the microchannel were affected by diffusion patterns generated from the microchannel (Fig. 4). As compared to the shear stress in a microfabricated channel on a 2D surface, flow rate (2 μL min^{-1}) we used may not

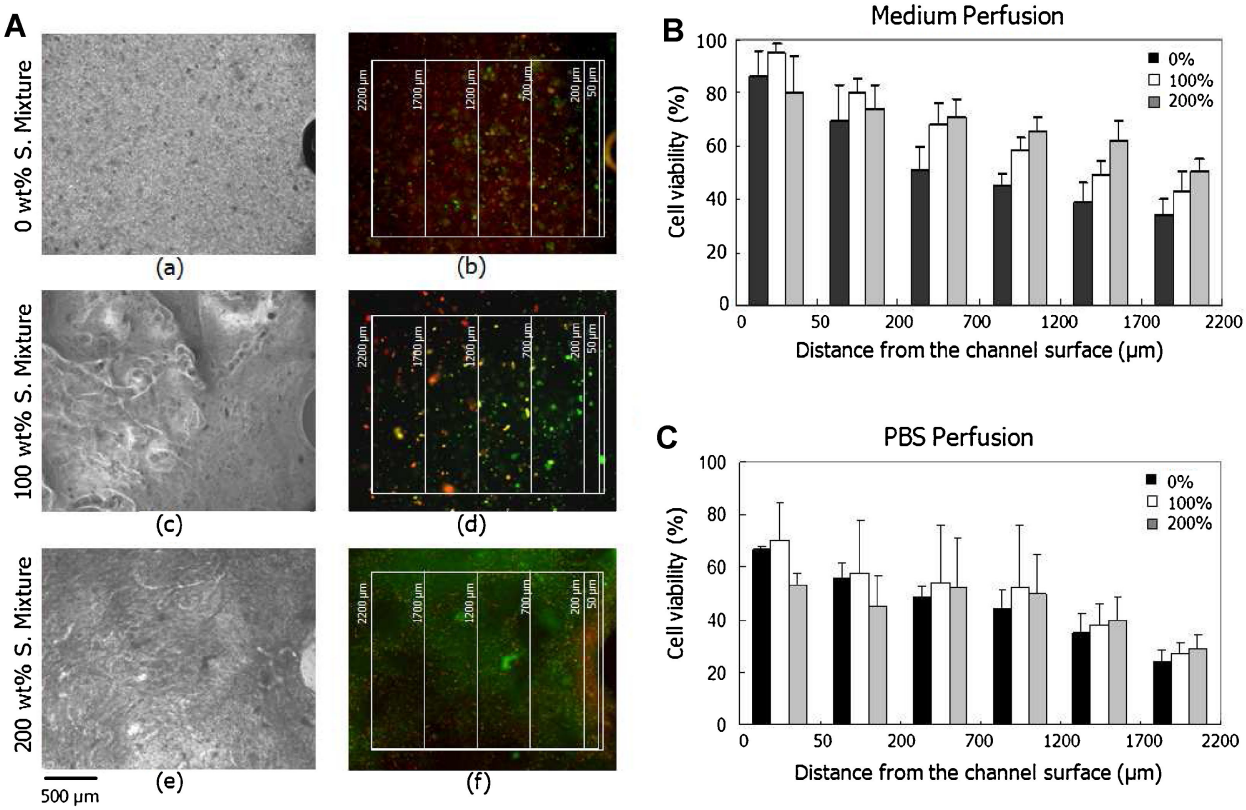

Figure 6. The viability of hepatic cells exposed to continuous medium perfusion from a microchannel within agarose gels. Cells were cultured in the agarose gel microchannel for 5 days in vitro. **A**: Phase contrast (**a**, **c**, and **e**) and fluorescent images (**b**, **d**, and **f**) of cells on the cross-sections in agarose gels with different sucrose concentrations (0–200 wt.%). The viability of the cells cultured for 5 days within the agarose gel channel with the medium perfusion (**B**) and PBS perfusion (**C**). The cell viability was analyzed and quantified as a function of the distance away from the microchannel surface. All quantification of the above data was performed three times for each condition. [Color figure can be seen in the online version of this article, available at www.interscience.wiley.com.]

significantly affect cell viability, because the hydrogel acts as a resistance of the fluidic flow, reducing flow penetration into the gel as it has been previously reported (Mosadegh et al., 2007).

To confirm the cell viability as a function of the distance away from the microchannel and assess the effect of oxygen and waste transfer on cell viability independent of the medium components, we analyzed cell viability in PBS perfusion condition (Fig. 6C). As expected, cell viability in a PBS perfusion condition was lower than the medium perfusion condition. Therefore, we demonstrated that pore sizes of agarose gels and variation of diffusion coefficient derived from the porosity played a significant role in influencing cell viability in a 3D cell-laden agarose gel device.

Conclusions

We developed a porous cell-laden hydrogel system with an engineered microporosity. Micropores were created by leaching sucrose crystals within cell-laden agarose gels and their distributions were controlled by varying sucrose concentrations (0–200 wt.%). We controlled and optimized the solubility of sucrose crystals and gelation time to improve physiological condition via a rapid cooling process. The microporosity (0–40%) was directly proportional whereas mechanical stiffness was inversely proportional to sucrose concentration. The diffusion of biomolecules in the porous gels was also analyzed as a function of the microporosity and the distance away from the microchannels. The diffusion coefficient in hydrogels derived from the formulation with 200 wt.% sucrose containing interconnected pores was 1.5 times higher as compared to non-porous agarose gels. We demonstrated that microporous structures significantly affected the diffusion of biomolecules and the viability of cells cultured within microporous cell-laden agarose gels. Cell viability in the porous agarose gel microchannels (200 wt.% sucrose) was 10–20% higher than in the non-porous agarose microchannels. Therefore, this approach may be potentially beneficial for engineering tissue constructs for regenerative medicine and drug discovery applications.

This article was partly supported by the National Institutes of Health (DE019024, HL092836, and EB007249), US Army Core of Engineers, and the Charles Stark Draper Laboratory. Jae Hong Park was supported by the Korea Research Foundation Grant funded by the Korean Government (MOEHRD) (Grant Number: KRF-2007-357-D00101). Bong Geun Chung was partially supported by the National Research Foundation of Korea (Grant Number R11-2008-044-01001-0) and Korea Industrial Technology Foundation (KOTEF) through the Human Resource Training Project for Strategic Technology.

References

Aymard P, Martin DR, Plucknett K, Foster TJ, Clark AH, Norton IT. 2001. Influence of thermal history on the structural and mechanical properties of agarose gels. Biopolymers 59(3):131–144.

Bakshi A, Fisher O, Dagci T, Himes BT, Fischer I, Lowman A. 2004. Mechanically engineered hydrogel scaffolds for axonal growth and angiogenesis after transplantation in spinal cord injury. J Neurosurg Spine 1(3):322–329.

Bignon A, Chouteau J, Chevalier J, Fantozzi G, Carret JP, Chavassieux P, Boivin G, Melin M, Hartmann D. 2003. Effect of micro- and macroporosity of bone substitutes on their mechanical properties and cellular response. J Mater Sci Mater Med 14(12):1089–1097.

Bryant SJ, Anseth KS. 2003. Controlling the spatial distribution of ECM components in degradable PEG hydrogels for tissue engineering cartilage. J Biomed Mater Res A 64(1):70–79.

Burdick JA, Anseth KS. 2002. Photoencapsulation of osteoblasts in injectable RGD-modified PEG hydrogels for bone tissue engineering. Biomaterials 23(22):4315–4323.

Burdick JA, Mason MN, Hinman AD, Thorne K, Anseth KS. 2002. Delivery of osteoinductive growth factors from degradable PEG hydrogels influences osteoblast differentiation and mineralization. J Control Release 83(1):53–63.

Burdick JA, Frankel D, Dernell WS, Anseth KS. 2003. An initial investigation of photocurable three-dimensional lactic acid based scaffolds in a critical-sized cranial defect. Biomaterials 24(9):1613–1620.

Cabodi M, Choi NW, Gleghorn JP, Lee CS, Bonassar LJ, Stroock AD. 2005. A microfluidic biomaterial. J Am Chem Soc 127(40):13788–13789.

Changez M, Koul V, Krishna B, Dinda AK, Choudhary V. 2004. Studies on biodegradation and release of gentamicin sulphate from interpenetrating network hydrogels based on poly(acrylic acid) and gelatin: In vitro and in vivo. Biomaterials 25(1):139–146.

Choi NW, Cabodi M, Held B, Gleghorn JP, Bonassar LJ, Stroock AD. 2007. Microfluidic scaffolds for tissue engineering. Nat Mater 6(11):908–915.

Cordell JM, Vogl ML, Wagoner Johnson AJ. 2009. The influence of micropore size on the mechanical properties of bulk hydroxyapatite and hydroxyapatite scaffolds. J Mech Behav Biomed Mater 2(5):560–570.

Cornelissen LH, Bronneberg D, Oomens CW, Baaijens FP. 2008. Diffusion measurements in epidermal tissues with fluorescent recovery after photobleaching. Skin Res Technol 14(4):462–467.

Elisseeff J, McIntosh W, Anseth K, Riley S, Ragan P, Langer R. 2000. Photoencapsulation of chondrocytes in poly(ethylene oxide)-based semi-interpenetrating networks. J Biomed Mater Res 51(2):164–171.

Fatin-Rough N, Starchev K, Buffle J. 2004. Size effects of diffusion processes within agarose gels. Biophysical J 86(5):2710–2719.

Ford MC, Bertram JP, Hynes SR, Michaud M, Li Q, Young M, Segal SS, Madri JA, Lavik EB. 2006. A macroporous hydrogel for the coculture of neural progenitor and endothelial cells to form functional vascular networks in vivo. Proc Natl Acad Sci USA 103(8):2512–2517.

Gillette BM, Jensen JA, Tang B, Yang GJ, Bazargan-Lari A, Zhong M, Sia SK. 2008. In situ collagen assembly for integrating microfabricated three-dimensional cell-seeded matrices. Nat Mater 7(8):636–640.

Golden AP, Tien J. 2007. Fabrication of microfluidic hydrogels using molded gelatin as a sacrificial element. Lab Chip 7(6):720–725.

Huang YC, Connell M, Park Y, Mooney DJ, Rice KG. 2003. Fabrication and in vitro testing of polymeric delivery system for condensed DNA. J Biomed Mater Res A 67(4):1384–1392.

Hwang CM, Khademhosseini A, Park Y, Sun K, Lee SH. 2008. Microfluidic chip-based fabrication of PLGA microfiber scaffolds for tissue engineering. Langmuir 24(13):6845–6851.

Khademhosseini A, Langer R. 2007. Microengineered hydrogels for tissue engineering. Biomaterials 28(34):5087–5092.

Khademhosseini A, Langer R, Borenstein J, Vacanti JP. 2006. Microscale technologies for tissue engineering and biology. Proc Natl Acad Sci USA 103(8):2480–2487.

Kwok KY, Adami RC, Hester KC, Park Y, Thomas S, Rice KG. 2000. Strategies for maintaining the particle size of peptide DNA condensates following freeze-drying. Int J Pharm 203(1–2):81–88.

Labille J, Fatin-Rouge N, Buffle J. 2007. Local and average diffusion of nanosolutes in agarose gel: The effect of the gel/solution interface structure. Langmuir 23(4):2083–2090.

Lee KY, Mooney DJ. 2001. Hydrogels for tissue engineering. Chem Rev 101(7):1869–1879.

Ling Y, Rubin J, Deng Y, Huang C, Demirci U, Karp JM, Khademhosseini A. 2007. A cell-laden microfluidic hydrogel. Lab Chip 7(6):756–762.

Linnes MP, Ratner BD, Giachelli CM. 2007. A fibrinogen-based precision microporous scaffold for tissue engineering. Biomaterials 28(35):5298–5306.

Liu Tsang V, Chen AA, Cho LM, Jadin KD, Sah RL, DeLong S, West JL, Bhatia SN. 2007. Fabrication of 3D hepatic tissues by additive photopatterning of cellular hydrogels. FASEB J 21(3):790–801.

Mann BK, Gobin AS, Tsai AT, Schmedlen RH, West JL. 2001. Smooth muscle cell growth in photopolymerized hydrogels with cell adhesive and proteolytically degradable domains: Synthetic ECM analogs for tissue engineering. Biomaterials 22(22):3045–3051.

Mosadegh B, Huang C, Park JW, Shin HS, Chung BG, Hwang SK, Lee KH, Kim HJ, Brody J, Jeon NL. 2007. Generation of stable complex gradients across two-dimensional surfaces and three-dimensional gels. Langmuir 23(22):10910–10912.

Murphy WL, Dennis RG, Kileny JL, Mooney DJ. 2002. Salt fusion: An approach to improve pore interconnectivity within tissue engineering scaffolds. Tissue Eng 8(1):43–52.

Nicholson C. 2001. Diffusion and related transport mechanisms in brain tissue. Rep Prog Phys 64:815–884.

Nicholson C, Phillips JM. 1981. Ion diffusion modified by tortuosity and volume fraction in the extracellular microenvironment of the rat cerebellum. J Physiol 321:225–257.

Nicholson C, Tao L. 1993. Hindered diffusion of high molecular weight compounds in brain extracellular microenvironment measured with integrative optical imaging. Biophys J 65(6):2277–2290.

Peppas NA, Hilt JZ, Khademhosseini A, Langer R. 2006. Hydrogels in Biology and Medicine: From Molecular Principles to Bionanotechnology. Advanced Materials 18(11):1345–1360.

Pluen A, Netti PA, Jain RK, Berk DA. 1999. Diffusion of macromolecules in agarose gels: Comparison of linear and globular configurations. Biophysical J 77(1):542–552.

Rahfoth B, Weisser J, Sternkopf F, Aigner T, von der Mark K, Brauer R. 1998. Transplantation of allograft chondrocytes embedded in agarose gel into cartilage defects of rabbits. Osteoarthritis Cartilage 6(1):50–65.

Shi QH, Zhou X, Sun Y. 2005. A novel superporous agarose medium for high-speed protein chromatography. Biotechnol Bioeng 92(5):643–651.

Song YS, Lin RL, Montesano G, Durmus NG, Lee G, Yoo SS, Kayaalp E, Haeggstrom E, Khademhosseini A, Demirci U. 2009. Engineered 3D tissue models for cell-laden microfluidic channels. Anal Bioanal Chem 395(1):185–193.

Sopyan I, Mel M, Ramesh S, Khalid KA. 2007. Porous hydroxyapatite for artificial bone applications. Sci Technol AdvMater 8(1–2):116–123.

Thorne RG, Nicholson C. 2006. In vivo diffusion analysis with quantum dots and dextrans predicts the width of brain extracellular space. Proc Natl Acad Sci USA 103(14):5567–5572.

Tian WM, Hou SP, Ma J, Zhang CL, Xu QY, Lee IS, Li HD, Spector M, Cui FZ. 2005. Hyaluronic acid-poly-D-lysine-based three-dimensional hydrogel for traumatic brain injury. Tissue Eng 11(3–4):513–525.

Uludag H, De Vos P, Tresco PA. 2000. Technology of mammalian cell encapsulation. Adv Drug Deliv Rev 42(1–2):29–64.

Woerly S. 1993. Hydrogels for neural tissue reconstruction and transplantation. Biomaterials 14(14):1056–1058.

Wu DQ, Sun YX, Xu XD, Cheng SX, Zhang XZ, Zhuo RX. 2008. Biodegradable and pH-sensitive hydrogels for cell encapsulation and controlled drug release. Biomacromolecules 9(4):1155–1162.

Zhou J, Zhou M, Caruso RA. 2006. Agarose template for the fabrication of macroporous metal oxide structures. Langmuir 22(7):3332–3336.